2014-09

Grazing angle photoluminescence of porous alumina as an analytical transducer for gaseous ethanol detection

Journal of Nanoscience and Nanotechnology, Valencia : American Scientific Publishers - ASP, v. 14, n. 9, p. 6653-6657, Sept. 2014
http://www.producao.usp.br/handle/BDPI/50749

Article

Journal of
Nanoscience and Nanotechnology
Vol. 14, 6653–6657, 2014
www.aspbs.com/jnn

Grazing Angle Photoluminescence of Porous Alumina as an Analytical Transducer for Gaseous Ethanol Detection

Haroldo A. Guerreiro[1, 2], Francisco Trivinho-Strixino[3], Adenilson J. Chiquito[2], Francisco E. G. Guimarães[4], and Ernesto C. Pereira[5, *]

[1] Department of Física, Institute of Ciências Exatas, University of Federal do Amazonas, 69077-000, Manaus-AM, Brazil
[2] Department of Física, University of Federal de São Carlos, 13565-905, São Carlos-SP, Brazil
[3] Department of Fís., Quím. e Mat., University of Federal de São Carlos-Campus Sorocaba, 18052-780, Sorocaba-SP, Brazil
[4] Instituto de Física de São Carlos, University of de São Paulo, 13560-970, São Carlos-SP, Brazil
[5] LIEC, Departamento de Química, University of Federal de São Carlos, 13565-905, São Carlos–SP, Brazil

Porous alumina was used to build an optical sensor for gaseous ethanol detection. The photoluminescence collected in a grazing angle was used as a transducer signal. The photoluminescence detected with this optical setup shows well resolved Fabry-Pérot type interference fringes at room temperature, whose position and shape are strongly dependent on the ethanol fraction adsorbed on the porous alumina surface. According to the surface porous morphology, different finesse and resolution between the emission fringes were observed. The analytical response of the sensor was tested in terms of spectral displacement of the fringes when in contact with gaseous ethanol. The sensor was tested for different temperatures and at 25 °C it presented the highest sensibility. The difference in the sensibility is a function of the temperature and can be related both to the modification of ethanol vapor pressure and the kinetics of adsorption processes at the walls of the glass cell and the porous alumina sample.

Keywords: Porous Alumina, Photoluminescence, Optical Sensor, Gas Sensor, Ethanol Detection.

1. INTRODUCTION

Porous Alumina (PA) with an almost perfect self-ordered hexagonal nanopores can be obtained by aluminum anodisation by using the two step preparation method.[1] This material has brought up great interest in diverse technological areas due to its singular porous characteristics[2] and suitable optical properties[3–7] which combine large surface/volume ratios with transparence and light emission in the near UV and visible range. In this sense, researchers have investigated promising candidates of substrates to use in optical sensor systems.[8–11] The advantages of these low dimension materials are the possibility to decrease the limit detection range and to build up new lab on a chip devices. The optical sensor based on this idea can work recording changes in the optical properties caused by light propagation in the nanoporous films and this effect could then be used to detect target compounds upon modifications of Fabry-Pérot fringes, photonic band gap (PBG), Bragg diffraction, and waveguide modes.[5, 9, 11, 12] These optical properties are very sensitive to minimal changes of the effective refractive index of the nanoporous material which are induced by target molecules anchored on the pore surface or filling the porous cavities with a specific exposed chemical environment. In this sense, an optical sensor having a nanoporous film as optical transducers is promising for sensing gaseous reactants. However, the directly record of refractive index variation requires sophisticated and expensive experimental apparatus.[7, 13] To overcome this technological drawback, we recently reported a different optical setup that records interference fringes in the UV and visible photoluminescence (PL) signal which propagates in limit grazing angle parallel to the porous alumina surface and orthogonal to the porous direction.[5] This approach allowed us to detect small quantities of pesticide content in a solution deposited over a bare porous alumina/aluminum substrate. The high sensitivity of this optical setup is related to the wavelength shift of the interference fringes that presents the same properties as those observed in a Fabry-Pérot cavity due to changes in the effective refractive index of the porous material.

*Author to whom correspondence should be addressed.

In this essay, we describe the use of this optical setup on porous alumina/aluminum substrate to detect small quantities of pure ethanol in the gas phase.

2. EXPERIMENTAL PROCEDURE

Aluminum substrates (99,99%, 0.02 in. thick, Alpha-Aesar) were cut in flag shape pieces with an exposed area of 1.2 cm^2. Prior to the experiments, the working electrode was mechanically abraded subsequently with #400 SiC, #600 SiC and then with #1200 SiC sandpaper followed by deionised water washes. After that, substrates were electrochemically polished in a solution of $HClO_4$ and C_2H_5OH (v:v-25:75) at 1 °C applying 15 V for 5 minutes. The porous alumina samples were grown under a galvanostatic regime (5 mA/cm^2) on an aluminum substrate in 120 mL of electrolyte solution containing 0.1 or 0.3 mol L^{-1} $H_2C_2O_4$ for 1500 or 2400 seconds. Only one anodisation step was performed. All solutions were prepared with deionised water and analytical-grade reagents. The electrolytic cell was maintained at 20 °C using a thermostatic circulating bath and the electrolyte solution was stirred using a magnetic stirrer. Two parallel Pt sheets were used as counter electrodes in order to obtain a homogeneous electric field distribution over the electrode surfaces. Pore widening was performed after anodisation in a H_3PO_4 solution at 65 °C for 25 minutes. A complete set of experimental parameters used to prepare the PA sample can be found in Table I. A lab made DC power supply was used to perform the experiments. The voltage was recorded using a HP-Agilent model 3440A Digital Multimeter connected to a computer by an inhouse written software routine using the HP-VEE® 5.0 software. The morphological characterization of the porous films was performed in a SEM Zeiss Supra 35VP using the ImageJ® software to analyze the images.

Table I. Experimental conditions used to prepare sample A, B and C.

Sample	Electrolyte	Concentration (Mol/L)	Temperature (°C)	Current density (mA/cm^2)	Anodisation time (s)	Pore widening
A	Oxalic acid	0.3	20	5	1500	No
B	Oxalic acid	0.3	20	5	2400	No
C	Oxalic acid	0.1	20	5	2400	Yes

A sealed glass cell (97 mL) with two quartz windows was specially designed to be used in an orthogonal excitation/detection configuration and was attached to a fluorescence spectrometer (Shimadzu fluorimeter, model RF-5301 connected to a computer) accordingly to Figure 1. The cell contains an inner sample chamber that allows the injection of ethanol aliquots and N_2 flux—for washing—after each essay. Pre-heated water was passed through an outer chamber to control the cell temperature. Monochromatic light at 340 nm was used for the excitation. The emission was collected in a grazing angle and a polarizer film was positioned in front of the emission window to separate the polarized component (orthogonal to the sample surface) before being detected. The PA film was positioned at the centre of this glass cell and the angle was adjusted to the highest PL intensity in the grazing PL setup.

3. RESULTS AND DISCUSSION

Figure 2 depicted the PA films morphology for three samples prepared under different experimental conditions, described in Table I. All samples have opened pores and a hexagonally array of periodically organized nanopores underneath the PA surface were observed (see graphs in Ref. Trivinho-Strixino et al.[5]). These images were analyzed and the pore size distributions for the samples A, B and C are shown in Figure 3. Samples A and B present almost the same average pore size (∼11 nm) while sample C has the largest average pore radius (∼25 nm).

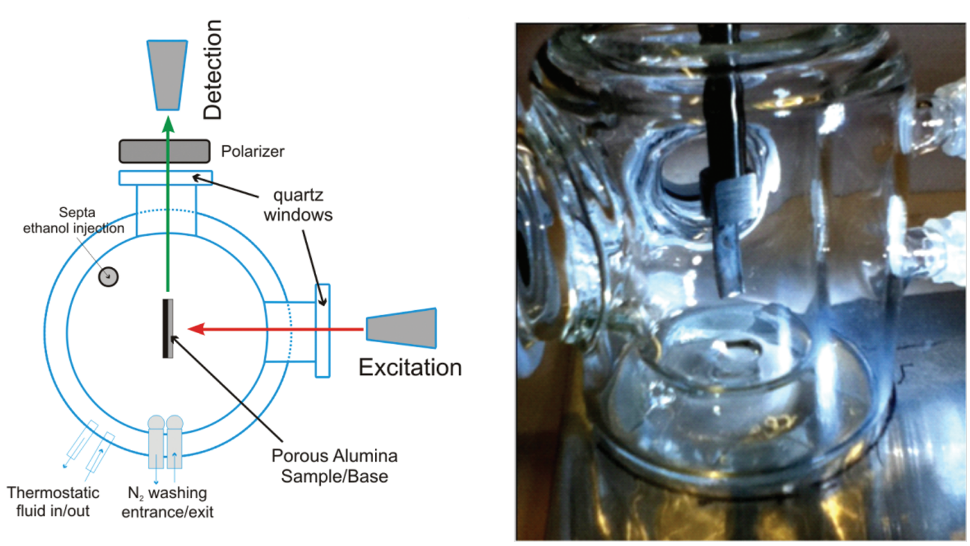

Figure 1. Experimental setup used to collect PL of PA samples at the grazing angle.

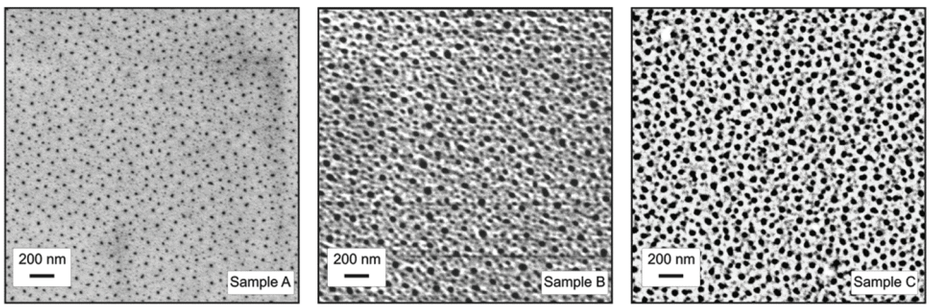

Figure 2. SEM images showing the top morphology of samples prepared at different experimental conditions depicted in Table I.

As described in the experimental section, it is important to stress out that the observed difference in the morphology is related only to the change in the experimental parameters used during the anodisation. Anodisation of sample A and B was carried out in a higher concentration of oxalic acid (0.3 mol/L) which might increase the dissolution rate inside the pores during the porous formation.[14] Sample B had been anodised for a longer time than sample A, and, as a consequence, this sample depicted a large porous radii distribution (Fig. 3). On the other hand, sample C was anodised in a lower oxalic acid concentration (0.1 mol/L) which might originate a pore with small radii values. However, this sample passed through an additional opening pore procedure (Table I), producing an increase on the average pore size, which leads to the observed large pore radii distribution (Fig. 3). The typical thickness of the porous layer, for samples B and C, is of 2 μm.[14] Since anodisation of sample A took less time (1500 s) than sample B and C (2400 s) under constant current density, it is expected the thickness of the porous layer of this sample to be about 1.2 μm.[14]

Figure 4 shows the typical grazing angle emission for PA/Al samples A, B and C detected at room temperature under air atmosphere. The three PL spectra under this optical condition are characterized by a broad emission band ranging from 350 nm to 670 nm, which is modulated by well resolved interference fringes. The interference is a result of multi reflections of the emitted light in the PA at the PA/Al and at the PA/gas parallel interfaces.[15] The wavelength λ of the fringe of order m (integer) depends on the effective diffraction index n_{eff} and on the PA thickness L as given by the following relation:

$$m\lambda = n_{\text{eff}} L \tag{1}$$

The value n_{eff} is close to the PA diffraction index value ($n_{\text{PA}} \sim 1.67$). Because the experimental optical setup used here, n_{eff} has small contributions of the diffraction indexes of the adsorbed gas material (n_{ad}) on the PA surface and of the gas material (n_{gas}) inside the PA pores and filling the sample chamber. To produce a $\Delta\lambda$wavelength variation, equal to 1 nm on the first order fringe ($m = 1$), the variation of the effective diffraction index Δn_{eff} should be somewhat 5×10^{-4} for a PA thickness of 2 μm. This value is within the range of ethanol vapor diffraction index ($n_{\text{gas}} \sim 0.0008$). Of course, the exchange of gases between air and ethanol inside the sample chamber could produce such a 1 nm shift of the fringe, but Δn_{eff} will be necessarily higher if we compute the contribution of the adsorbed gas molecules on the PA surface.

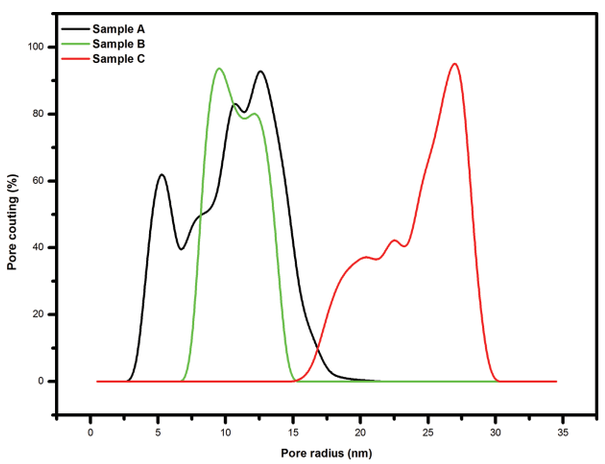

Figure 3. Morphology analysis of porous radius distribution for samples prepared at different experimental conditions depicted in Table I.

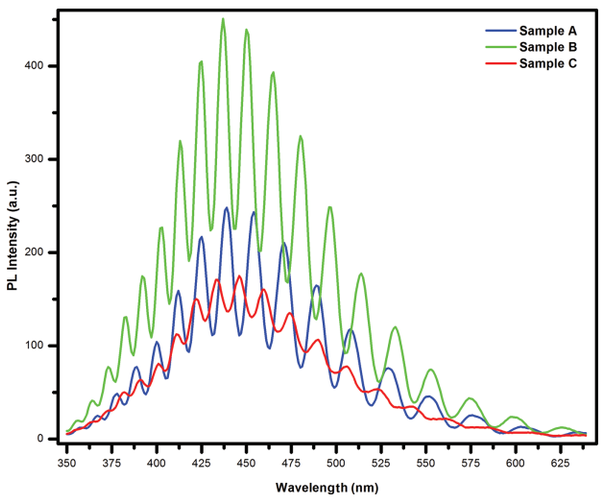

Figure 4. PL spectra collected at a grazing angle for the three samples. Effect of the PA morphology on the photoluminescence.

The differences in the PL spectra depicted in Figure 4 show how the sample morphology affects the interferometric behavior of the PA/Al system. The major differences of the three samples were: the thickness L of porous layer, the average pore diameter and the film quality, in terms of roughness and transparence. Although sample C showed a weak finesse from the interferometric optical component, we chose it because it had the largest pores diameter distribution among the three samples. We believe that the larger surface contact with ethanol molecules the more sensitive the PA/Al system can be for gaseous detection.

In order to start the analytical study, we needed to choose the better transducer signal for this case. The photoluminescence properties depicted in this system collected in a grazing angle were very rich when in contact with the ethanol gaseous molecules. Few minutes after injections of liquid ethanol aliquots, we observed several PL spectra modifications, such as changes in the fringes intensities, spectral displacement of the fringes wavelength maximum and the variation of the full width at half maximum of all fringes. These modifications are probably related to a variation of the medium refractive index or a variation of active PL sites at the porous surface when in contact with different gaseous molecules.[16–19] The latter statement needs more scientific data to be proved. In the sense of an analytical purpose to build an optical sensor, it is possible to choose any of these PL modifications as the transducer signal if that response is a function of the molecules quantity we want to determine. In the present case, we chose the lateral displacement of the fringes wavelength maximum of one specific fringe (the most intense) as a transducer signal, once this signal showed great interaction with the ethanol gaseous molecules injected in the glass cell.

To test the optical sensor capability of the PA/Al system we performed a first essay related to kinetics properties of the sensor when in contact with gaseous ethanol. The PL spectra presented in Figure 5 portrays the emission spectra of PA/Al collected at different time intervals after the injection of 100 μL of ethanol inside the glass cell. The fringe structure and intensity of the PL spectra had continuously changed for 15 minutes of ethanol evaporation until it stabilized over the remaining 23 minutes of measurement. During the first 5 minutes of ethanol evaporation, we observed basically a continuous displacement of the fringes toward the red as given by the arrows in Figure 5, consequence of the effective diffraction index change. In addition, a small variation of the fringe resolution after 5 minutes of ethanol injection could be detected. After 15 minutes, the PL intensity, as well as the spectral displacement and resolution, stopped to change. Both fringe intensity and resolution are modified by the waveguide detuning, which produces losses due to changes of the effective diffraction index. The final spectral shift depends on the fringe order, as already given by Eq. (1), but it is close to the initial displacement between two consecutive fringes m and $m(+1)$ in the wavelength displacement for the highest intensity fringes that possess order values in the range of 15–20 and spectral distances close to 15 nm.

We consider that during the measurement elapsed time, the equilibration condition between gas and the maximum elapsed time for the sample C to be capable to detect 100 μL of ethanol in the gas phase throughout the glass cell volume (97 mL).

The following experiment was carried out at different temperatures inside the glass cell chamber and for sample C, each spectrum was collected after the injection of small aliquots of ethanol waiting time enough for its total evaporation. This allowed us to modify the ethanol vapor pressure during the experiments and so, to test the capability of the sensor when in contact with different ethanol vapor quantities.

Figure 6 showed the fringe displacement of the wavelength maximum collected in the range of 15 nm as a

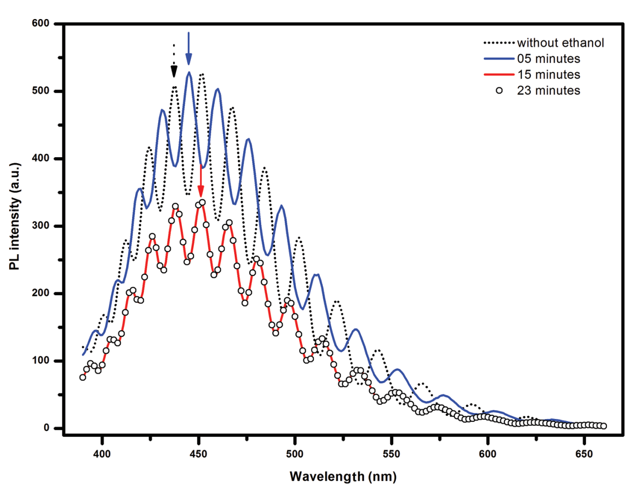

Figure 5. PL spectra collected at a grazing angle for sample C after injection of 100 μL of liquid ethanol inside the glass cell at different periods. Glass temperature was maintained at 25 °C.

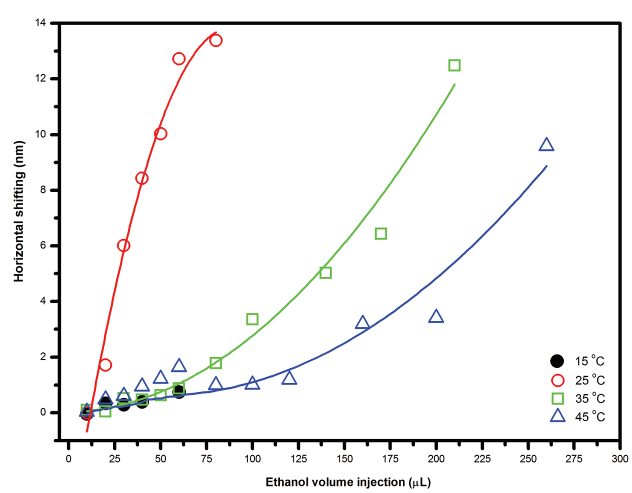

Figure 6. Horizontal shifting of the wavelength maximum of the most intense fringe for sample C after injection of different aliquots of liquid ethanol inside the cell kept at different temperatures.

function of ethanol volume injected inside the cell at different temperatures. From this figure, the experiment carried out at 25 °C (red circles) presented an almost linear increase of the fringe position as a function of the ethanol injected volume (0.2 nm/μL) up to 60 μL of ethanol and then stabilized when the fringe shift was close to the displacement of 15 nm between two consecutive fringes. This sensibility was detected after the first volume injection. However, the fringe shift presented two different behaviors for higher temperatures (35 °C and 45 °C): the fringes displaced slowly for the first volume injections and then a sharp onset was detected for larger volume injections of ethanol. For the experiment carried out at 35 °C, this onset emerged after 100 μL of ethanol injection with an apparent sensibility of 0.07 nm/μL, while the spectral shift sharply increased at rates of 0.045 nm/μL after ethanol injection 150 μL for the experiment at 45 °C. For the experiment carried out at 15 °C, the spectral shift reached the saturation at 15 nm, instantaneously after the first volume injection of 10 μL.

The few nanometers spectral displacement of the emission fringes in the range of low volume injection observed in Figure 6, for higher temperatures (35 °C and 45 °C), can be accounted for the increase of diffraction index in the gas phase (n_{gas}) due to the increase of the ethanol partial pressure inside the PA pores and the glass cell. In the ethanol volume range above the onset of the spectral shift, the partial pressure is high enough to produce the ethanol adsorption on the PA pore surface at equilibrium and, consequently, a substantial increase of the diffraction index component of the adsorbed gas material (n_{ad}). Considering that the adsorption of ethanol at the glass walls surface is negligible, changing the temperature inside the cell will cause variation on the equilibrium partial pressure necessary for the molecule adsorption, as can be observed in Figure 6. For the experiment carried out at 25 °C, the equilibrium partial pressure would cause molecular adsorption even at the first volume injection of ethanol. In this case, the spectral shift is mainly related to the change of (n_{ad}). It is interesting to see that the molecular coverage of the PA increases continuously with the increase of the equilibrium partial pressure. This behavior is more evident in the essay performed at 15 °C, since at this temperature the surface coverage is produced instantaneously and produces the saturation of spectral shift around 15 nm. At this point, it is difficult to establish a secure sensibility parameter of this optical sensor. Thereunto some experiments must be done using more accurately measurements of ethanol partial pressures taking into account the PA real contact surface area and also the wall of the chamber. Nevertheless, we are able to demonstrate the feasibility of this system to detect very small changes of gaseous ethanol molecules quantity over different ranges of temperature.

4. CONCLUSIONS

Samples of PA were synthesized in order to test their capability to be applied as optical sensors for gaseous ethanol detection. The PA photoluminescence collected in a grazing angle depicted an interferometric behavior similar to a Fabry-Pérot device. Samples with different porous morphology showed different finesse and PL shapes. The lateral shift of the fringes wavelength maximum was used as the transducer signal and the variation of the temperature during the detection of gaseous ethanol showed a polynomial increase behavior as a function of the injected ethanol volume. The sensor proposed here responded to very small changes in the ethanol partial pressure at different temperatures.

Acknowledgment: We gratefully acknowledge the financial support provided by CNPq and FAPESP (Proc. FAPESP 2010/10813-0, FAPESP 2010/07794-4 and FAPESP 2013/07296-2).

References and Notes

1. H. Masuda and K. Fukuda, *Science* 268, 1466 (**1995**).
2. M. Hasan, A. K. Kasi, J. K. Kasi, and N. Afzulpurkar, *Nanoscience and Nanotechnology Letters* 4, 569 (**2012**).
3. J.-I. Hahm, *Journal of Biomedical Nanotechnology* 9, 1 (**2013**).
4. Y. Fan, K. Hotta, A. Yamaguchi, and N. Teramae, *Opt. Express* 20, 12850 (**2012**).
5. F. Trivinho-Strixino, H. A. Guerreiro, C. S. Gomes, E. C. Pereira, and F. E. G. Guimaraes, *Appl. Phys. Lett.* 97, 011902 (**2010**).
6. H. Sakaue, T. Kuriki, and T. Miyazaki, *J. Lumin.* 132, 256 (**2012**).
7. A. Yamaguchi, K. Hotta, and N. Teramae, *Anal. Chem.* 81, 105 (**2009**).
8. K. Hotta, A. Yamaguchi, and N. Teramae, *J. Phys. Chem. C* 116, 23533 (**2012**).
9. A. Santos, V. S. Balderrama, M. Alba, P. Formentin, J. Ferre-Borrull, J. Pallares, and L. F. Marsal, *Nanoscale Research Letters* 7, 1 (**2012**).
10. A. Santos, G. Macias, J. Ferre-Borrull, J. Pallares, and L. F. Marsal, *Acs Applied Materials and Interfaces* 4, 3584 (**2012**).
11. S. D. Alvarez, C.-P. Li, C. E. Chiang, I. K. Schuller, and M. J. Sailor, *Acs Nano* 3, 3301 (**2009**).
12. T. Kurneria, M. D. Kurkuri, K. R. Diener, L. Parkinson, and D. Losic, *Biosens. Bioelectron.* 35, 167 (**2012**).
13. K. H. A. Lau, L.-S. Tan, K. Tamada, M. S. Sander, and W. Knoll, *J. Phys. Chem. B* 108, 10812 (**2004**).
14. G. D. Sulka, Highly ordered anodic porous alumina formation by self-organized anodizing, Nanostructured Materials in Electrochemistry, First edn., edited by A. Eftekhari, Wiley-VCH, Berlin (**2008**), p. 1.
15. C. Pacholski, M. Sartor, M. J. Sailor, F. Cunin, and G. M. Miskelly, *J. Am. Chem. Soc.* 127, 11636 (**2005**).
16. J. H. Chen, C. P. Huang, C. G. Chao, and T. M. Chen, *Appl. Phys. A: Mater. Sci. Process.* 84, 297 (**2006**).
17. Y. Han, L. Cao, F. Xu, T. Chen, Z. Zheng, K. Qian, and W. Huang, *Mater. Chem. Phys.* 129, 1247 (**2011**).
18. G. S. Huang, X. L. Wu, G. G. Siu, and P. K. Chu, *Solid State Commun.* 137, 621 (**2006**).
19. G. S. Huang, X. L. Wu, L. W. Yang, X. F. Shao, G. G. Siu, and P. K. Chu, *Appl. Phys. A: Mater. Sci. Process.* 81, 1345 (**2005**).

Received: 19 July 2013. Accepted: 17 September 2013.